Efficient diclofenac sodium removal from water using a stable MOFs

and accessible membrane separation method

Xiao-Jing Hu, Yu-Lin Li, Hai-Xiong Liu, Shao-Ming Ying*, Qi Yin* Tian-Fu Liu

1. Materials and Instrumentation

All the reagents and solvents were commercially available and used without further purification. Powder X-ray diffraction patterns (PXRD) were measured by using a Rikagu Miniflex 600 Benchtop X-ray diffraction instrument. N_2 sorption measurements were conducted on ASAP 2460 from Micromeritics Co. Ltd. All the samples underwent solvent exchange with acetone and activation at 100 °C for 12 h before N_2 sorption measurements. The morphologies of MOF nanoparticles were studied using scanning electron microscope (Zeiss Sigma 300) working at 10 KV. The concentrations of DCF were measured with a UV-vis spectrophotometer (UV-8000S, Shanghai Metash Instruments). Zeta-potential tests and size distribution analysis of MOF-808 particles were performed using a Malvern Zetasizer Nano ZS90. The Pore size and porosity of the obtained membranes were tested by Mercury intrusion porosimetry (Micromeritics Autopore V 9620).

2. Synthesis of MOF samples

MOF-808 has been synthesized by solvothermal reaction using a slightly modified procedure of previous reports.[1] First, H_3BDC (105 mg) was ultrasonically dissolved in DMF (22.5 ml) and placed in a Teflon-lined stainless-steel autoclave, then $ZrOCl_2 \cdot 8H_2O$ (385 mg) and formic acid (12.5 ml) were mixed into the solution by ultrasonic for fifteen minutes. The mixture was finally reacted under 130 °C for two days. After cooling to room temperature, the precipitated white powder was collected by centrifugation, washed several times with fresh DMF and soaked in DMF and acetone for three days, respectively. The acetone of MOF-808 was removed by evacuating under room temperature.

NU-1000, UiO-66 and $UiO-66-NH_2$ were prepared via solvothermal method according to the published procedure.[2] For the synthesis of NU-1000, 30 mg of $ZrOCl_2 \cdot 8H_2O$, 10 mg of H_4TBAPy, 300 mg of benzoic acid, and 2 mL of DMF were added to a 20 mL glass vial and heated in an electric oven for 24 h at 120 °C. For the synthesis of UiO-66 and $UiO-66-NH_2$, 160 mg of $ZrCl_4$, 114 mg H_2BDC or NH_2-BDC, and 40 mL of DMF were added to a Teflon-lined stainless-steel autoclave and heated in an electric oven for 48 h at 120 °C. After the synthesis, the resulting solid was filtered and purified with DMF

and acetone for three days, respectively. The products were dried in a vacuum oven at 100 °C for 12 h.

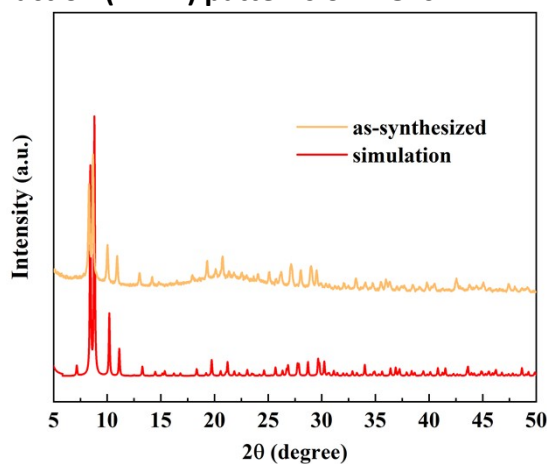### 3. Powder X-ray diffraction (PXRD) patterns of MOFs

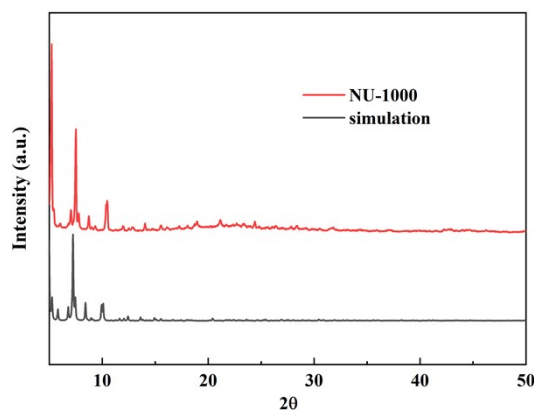Fig S1 PXRD patterns of the prepared MOF-808.
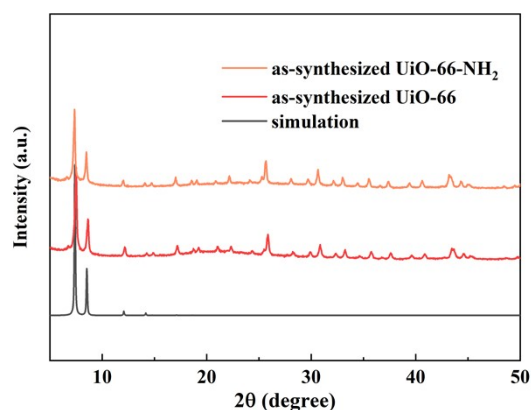

Fig S2 PXRD patterns of the prepared NU-1000.

Fig S3 PXRD patterns of the prepared UiO-66 and UiO-66-NH$_2$.

4. N$_2$ adsorption isotherms of MOF-808

Before N$_2$ sorption experiments, the as-synthesized MOF-808 samples were washed with N, N-Dimethylmethanamide (DMF) for several times and immersed in fresh DMF for 3 days, during which the solvent was decanted and freshly replenished three times.

Then, the samples were immersed in acetone for another 3 days to remove DMF moleculesin MOF, during which the solvent was decanted and freshly replenished three times. The solvent was removed and then activated at 100°C for 24 h under evacuation before measurements. Gas sorption measurements were then conducted using a Micrometritics ASAP 2460 system. N_2 sorption isotherms for MOF-808 are presented in Fig.S4.
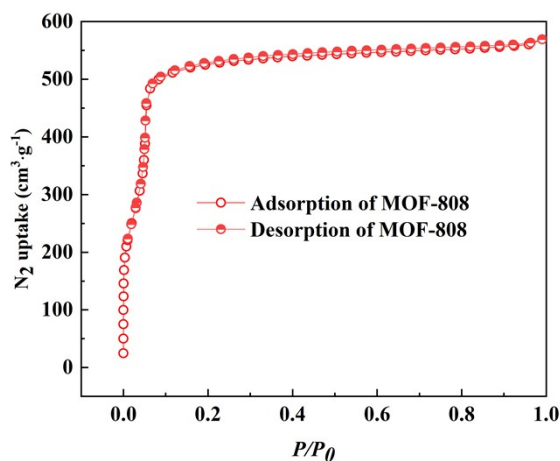

Fig S4 N_2 sorption isotherms at 77 K for prepared powdery MOF-808.

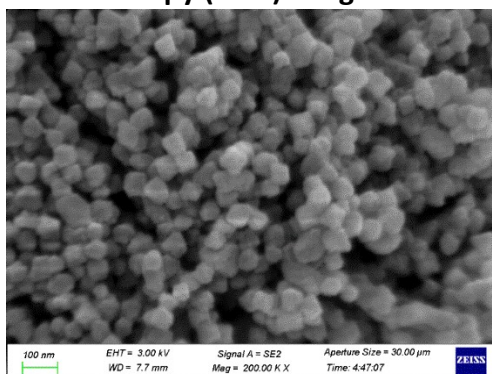## 5. The scanning electron microscopy (SEM) image of MOF-808

Fig S5 SEM image of MOF-808.

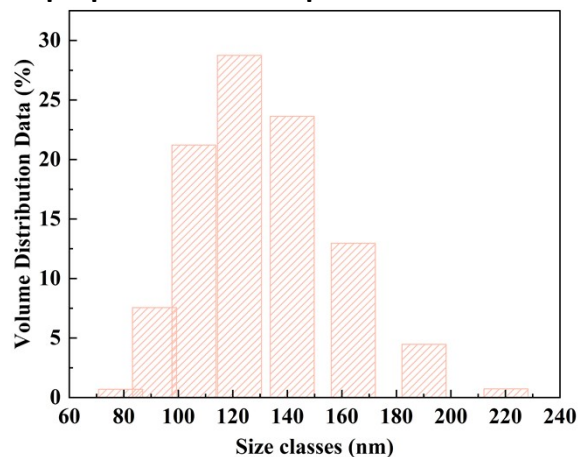## 6. Size distribution of prepared MOF-808 particles

Fig S6 size distribution of prepared MOF-808 particles.

7. PXRD patterns of MOF-808 related with water stability test

30 mg of sample was soaked in aqueous solution with different PH from 1 to 12 for 24 h. Then all the samples are centrifuged and washed with water and acetone for three times and dried directly in the air. Finally, those samples were characterized by powder X-ray diffraction.
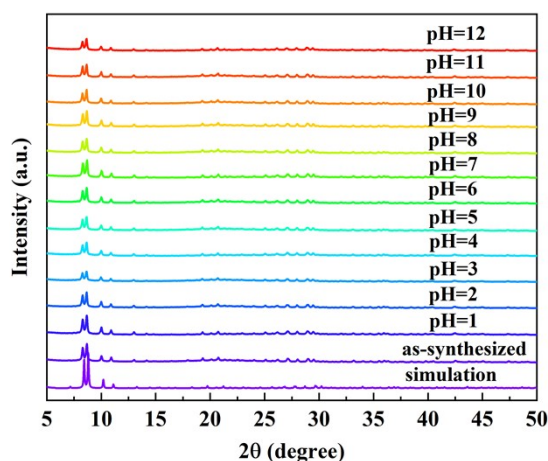

Fig S7 PXRD patterns of MOF-808 after being soaked in aqueous solution with pH.

8. Diclofenac adsorption studies on MOFs

8.1 Procedures for DCF calibration curve
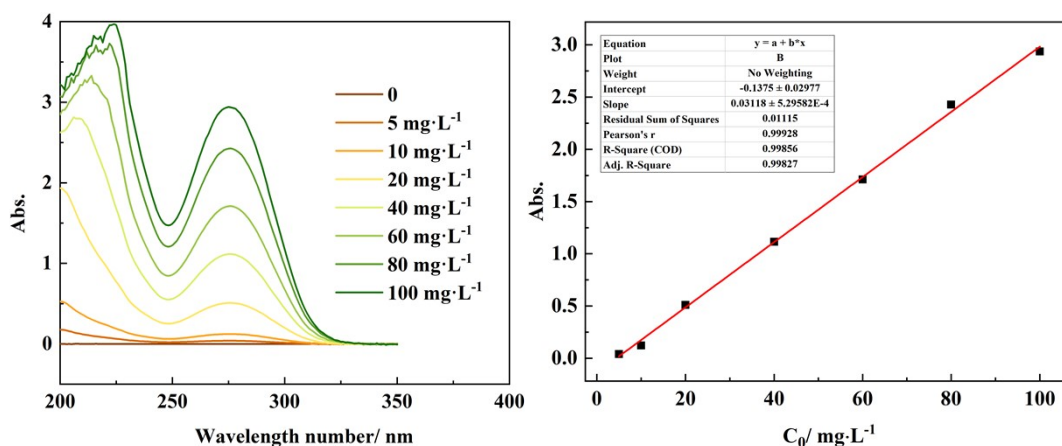
Fig S8 DCF calibration curve was obtained by determining the absorbance at 276 nm with a series of standard DCF solutions.

8.2 DCF adsorption isotherm experiment

Before adsorption isotherm experiment, the UV-vis spectra data of the original DCF solution was acquired. 100 ml of aqueous solution containing DCF (0, 20 mg·L^{-1}, 40 mg·L^{-1}, 60 mg·L^{-1}, 80 mg·L^{-1}, 100 mg·L^{-1}) was put in a capped conical flask and shaken in a shaking water bath for half an hour (150 rmp, 25 °C). And 10 mg of activated MOF-808 powder was subsequently added into each solution, and left undisturbed for three

hours. Afterwards, around 2.5 mL of solutions was filtered out by syringe filters and measured using an UV–vis spectrophotometer. Finally, the DCF concentration was determined from the absorbance of the UV spectrum and the calibration curve.

Langmuir model:

$$Q_e = \frac{K_L * Q_{max} * C_e}{1 + K_L * C_e} \qquad \text{Eq. (1)}$$

Freundlich model:

$$Q_e = K_F C_e^{1/n} \qquad \text{Eq. (2)}$$

where K_L and K_F was the kinetic constant of the Langmuir and Freundlich model, C_e was the equilibrium concentration of DCF, Q_e and Q_t was the DCF quantities adsorbed at equilibrium, Q_{max} of the Langmuir model was the maximum adsorption capacity, used to calculate the maximum adsorption capacity of MOF-808.

Table 1 Isothermal models parameters for DCF adsorption of MOF-808

Parameters / Models	Adsorption isothermal parameters			
	$K_L(\text{L·mg}^{-1})$	K_F	$Q_{max}(\text{mg g}^{-1})$	R^2
Freundlich		257		0.994
Langmuir	0.25		630	0.998

8.3 Comparison of various MOFs for diclofenac removal

Table 2 DCF adsorption capacity of different MOF adsorbents

Adsorbent	$Q_{max}(\text{mg g}^{-1})$	Refs.
18 %SO$_3$H-UiO-66	263	3
UiO-66-NH$_2$ (25)	357	4
Fe$_3$O$_4$@MIL-100(Fe)	400	5
MIL-53(Al)	422	6
UiO-66-(COOH)$_2$	480.5	7
PCN-206	490	8
{[Cu$_2$(L).(H$_2$O)$_2$](1.x solvent)}	490	9
MIL-101-Fe	544	10
UiO-66-NH$_2$ (90)	555	4
UiO-66-(COOCu)$_2$	624.3	7
MOF-808	630	This work

[Cu(BTTA)]n.2DMF	650	11
MIL-100-Fe	773	10
UiO-66-(COOFe)$_2$	796.1	7

8.4 DCF adsorption kinetics experiment

The time - depended DCF adsorption performance of MOF-808 was were studied in a time range of 0~120 min. Firstly, 100 ml of aqueous solution containing DCF (50 mg·L^{-1}) was put in a capped conical flask and shaken in a shaking water bath for half an hour (150 rmp, 25 °C), and 10 mg of activated MOF-808 powder was subsequently added into the solution. At a periodical time (5, 10, 20, 40, 60, 120 min), around 2.5 mL of supernatant was taken out and measured using an UV–vis spectrophotometer. Finally, the DCF concentration was determined from the absorbance of the UV spectrum and the calibration curve.

To determine the amount of adsorbed DCF, the following equations was used[3]:

$$q_t = (C_0 - C_t)\frac{v}{w}$$

where C_0 (mg·L^{-1}) is the initial concentration, C_t (mg·L^{-1}) is the concentration at time t, v (L) is the volume of the DCF solution and w (g) is the weight of the adsorbents.

The pseudo-first-order model and pseudo-second order models were tested to evaluate the kinetic adsorption process.

Pseudo-first-order model:

$$Q_t = Q_e * (1 - e^{-K*t}) \qquad \text{Eq. (3)}$$

Pseudo-second-order model:

$$\frac{t}{Q_t} = \frac{1}{K_2 * Q_e^2} + \frac{t}{Q_e} \qquad \text{Eq. (4)}$$

where Q_t (mg·g^{-1}) is the adsorption capacity at time t (min), K_2 (g·min^{-1}·mg^{-1}) is rate constants of pseudo-second order model, Q_e is the DCF adsorption capacity of equilibrium.

Table 3 Adsorption kinetic parameters of MOF-808 for DCF removal

Parameters	kinetics parameters		
Model	$Q_e(mg·g^{-1})$	K	R^2
Pseudo-first-order	424	0.079	0.977
Pseudo-second-order	483	2.09×10^{-4}	0.9865

8.5 DCF adsorption tests of other Zr-MOFs

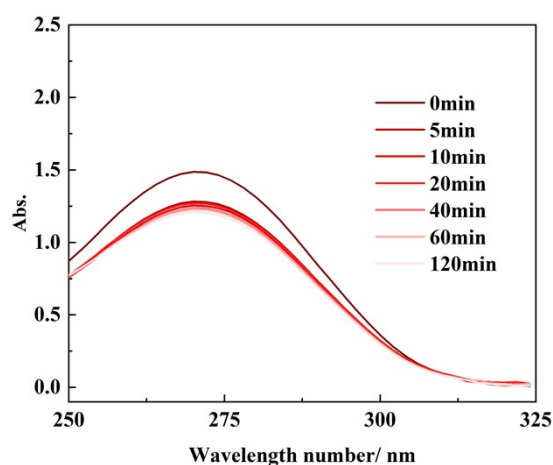The DCF adsorption experiment of NU-1000, UiO-66, and UiO-66-NH$_2$were similar with MOF-808.

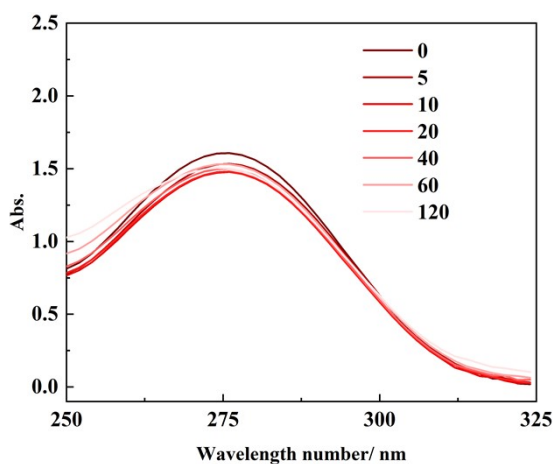Fig S9 Time-depended UV-vis spectra of DCF solution in the presence of UiO-66.

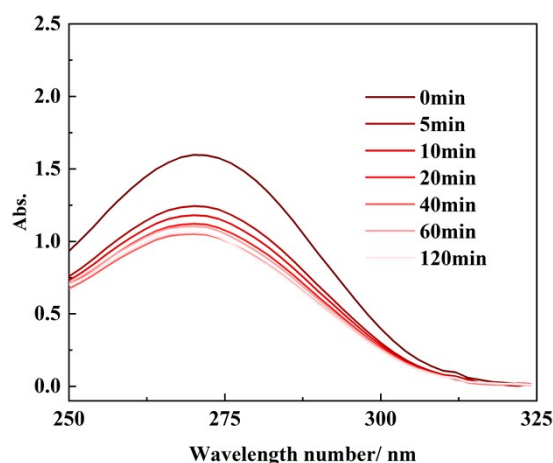Fig S10 Time-depended UV-vis spectra of DCF solution in the presence of UiO-66-NH$_2$.

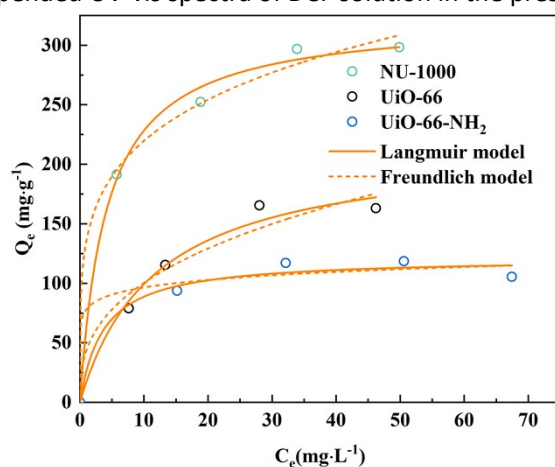Fig S11 Time-depended UV-vis spectra of DCF solution in the presence of NU-1000.

Fig S12 DCF adsorption isotherm of NU-1000, UiO-66, and UiO-66-NH$_2$.

Table 4 Isothermal models parameters for DCF adsorption of MOFs

Models Adsorbents	Langmuir			Freundlich	
	K_L($L \cdot mg^{-1}$)	Q_{max}(mg g^{-1})	R_L^2	K_F	R_F^2
NU-1000	0.24	323	0.994 (54)	135	0.994 (03)
UiO-66	0.08	216	0.979	43	0.951
UiO-66-NH$_2$	0.27	121	0.972	78	0.963

9. Synthesis and photos of membranes

The MOF-based MMMs could be easily fabricated by casting solution of MOF-808 particles and polymers onto a smooth glass plate, followed by solvent evaporation at room temperature to obtain a free-standing membrane. To prepare the casting mixtures, a certain mass of MOF-808 nanoparticles (0.1 g/0.2 g/0.3 g) and PAN (0.5 g) were initially dispersed in 5 mL DMF by stirring for twelve hours. Then the MOF and polymer solution was poured onto a flat glass surface and cast onto a membrane using a blade. After that, the membrane was dried at room temperature for about several

minutes. Finally, spray the membrane with industrial ethanol and separate it from the glass plate to obtain a free-standing membrane.
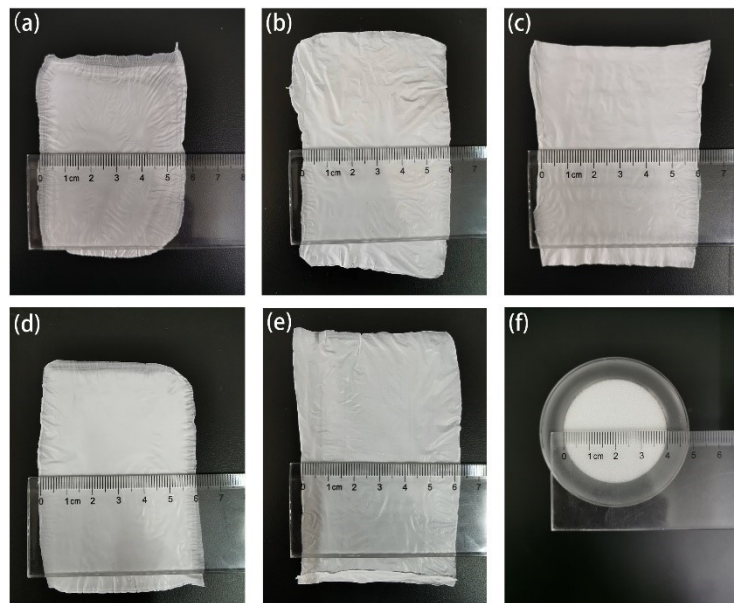

Fig S13 (a) PAN membrane; (b) M-20%; (c) M-40%; (d)M-60%; (e) M´-60%; (f) filter of vacuum filtration device.

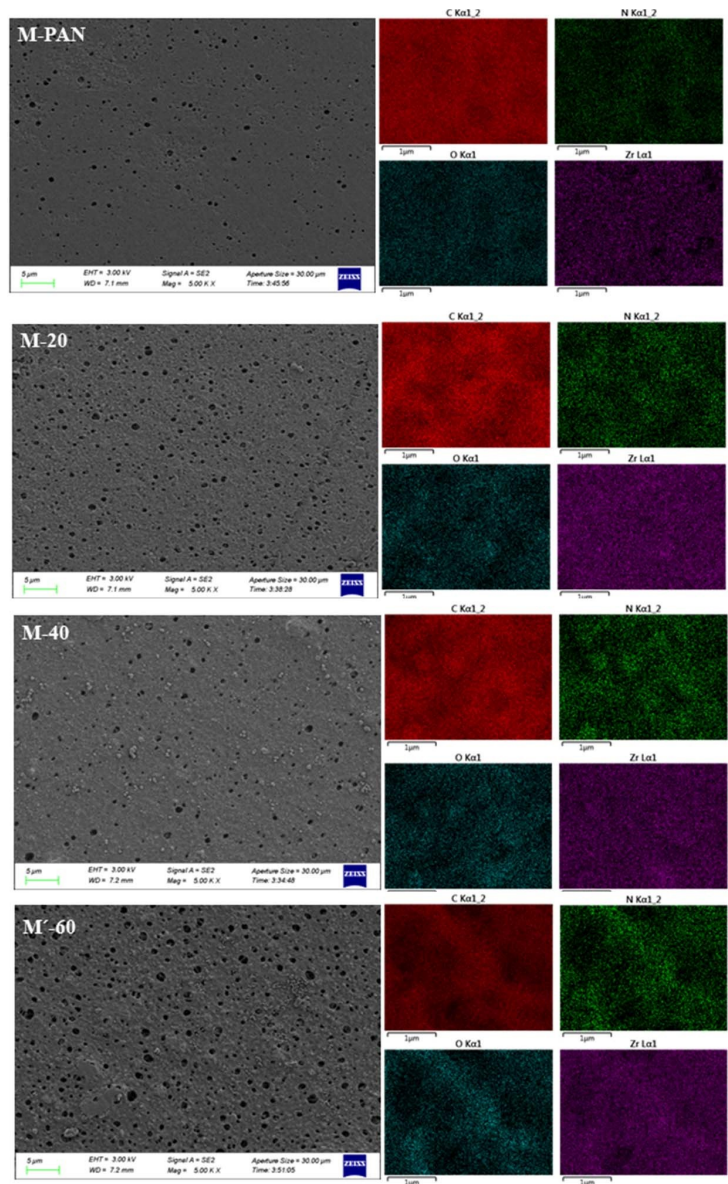## 10. The SEM image and EDS mapping of membranes

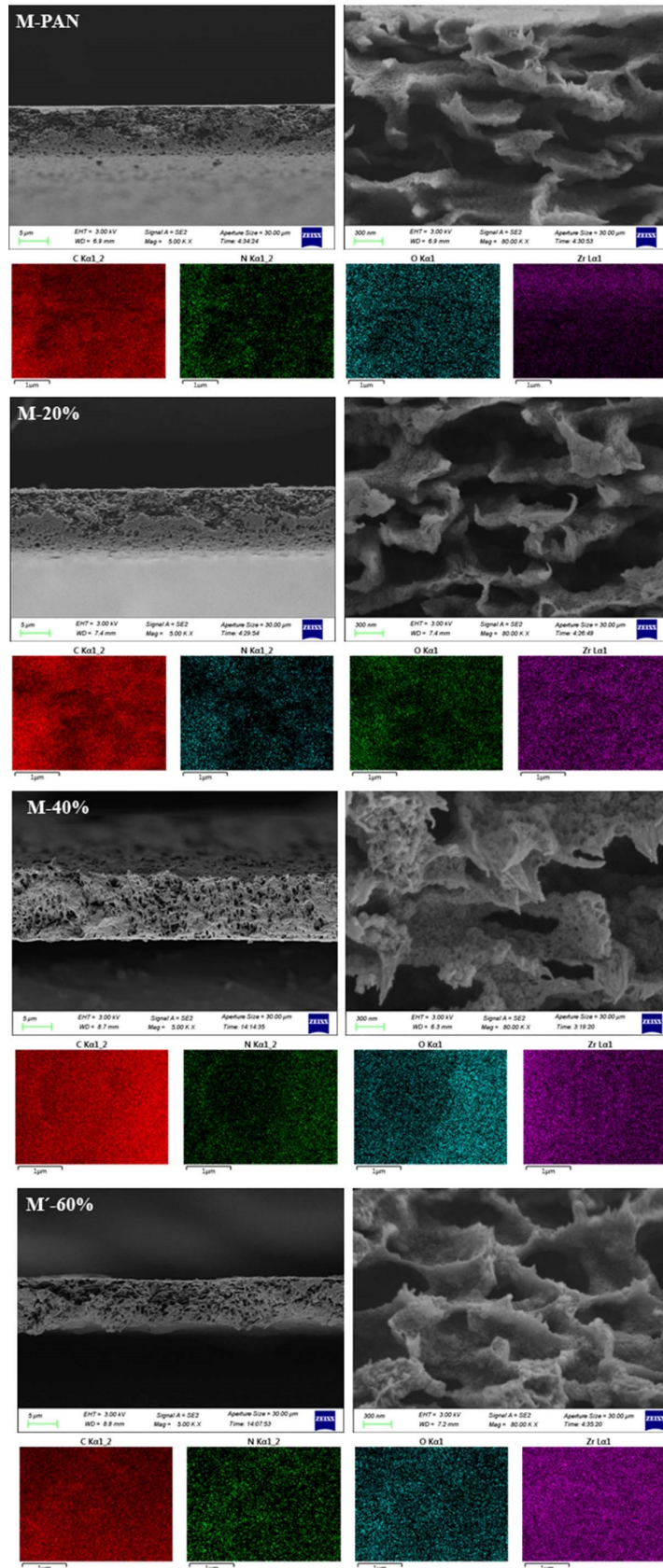Fig S14 Surface morphology and EDS mappings of as synthesized membranes.

Fig S15 Cross-sectional SEM images and EDS mapping of as synthesized membranes.

11. Photography of the bent state of MOF MMMs

Fig S16 Photography of the bent state of M-60%.

12. DCF removal study of MOFs membranes

A vacuum filter device was used to test DCF removal efficiency of membranes, and membranes were used as filters to extract DCF from aqueous solutions. All membranes were sandwiched between two sheets of filter paper, fixed in vacuum filter device, and flushed for three times with ultrapure water before applied to filter DCF solution.

Fig S17 Schematic diagram of the experimental device for DCF removal process based on membranes.

DCF removing efficiency (RE), the variation in DCF concentration before and after filtration, was employed to evaluating the performance of the obtained membranes, and calculated with the following equations:

$$RE(\%) = \frac{c_0 - c_f}{c_0} \times 100\% \qquad \text{Eq. S5}$$

where C_0 (mg·L^{-1}) is the initial concentration, C_f (mg·L^{-1}) is the concentration after five
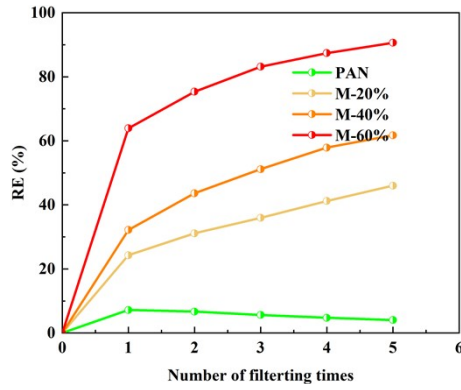
filtrations.

Fig S18 Removal efficiency of membranes from once to fifth filtration.
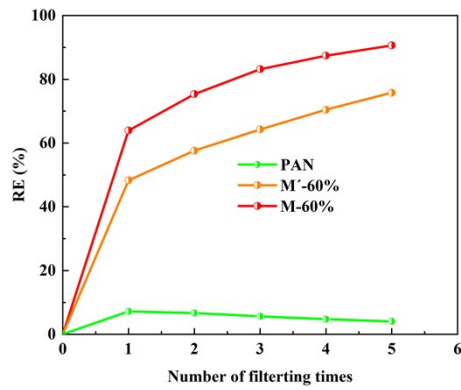

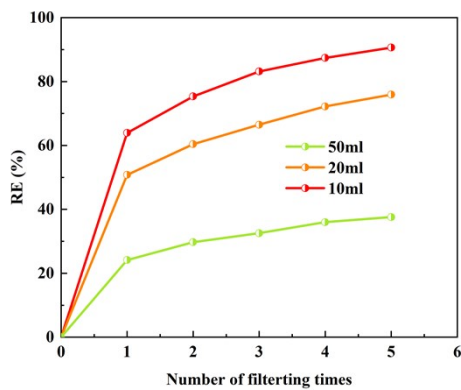Fig S19 Removal efficiency of membranes with different thickness from once to fifth filtration.

Fig S20 Removal efficiency of M-60% for different volume of DCF solution from once to fifth
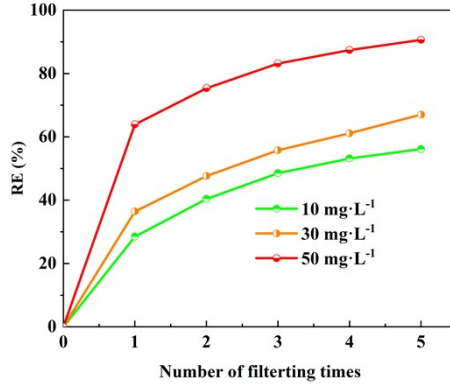
filtration.

Fig S21 Removal efficiency of M-60% for different DCF concentration from once to fifth filtration.

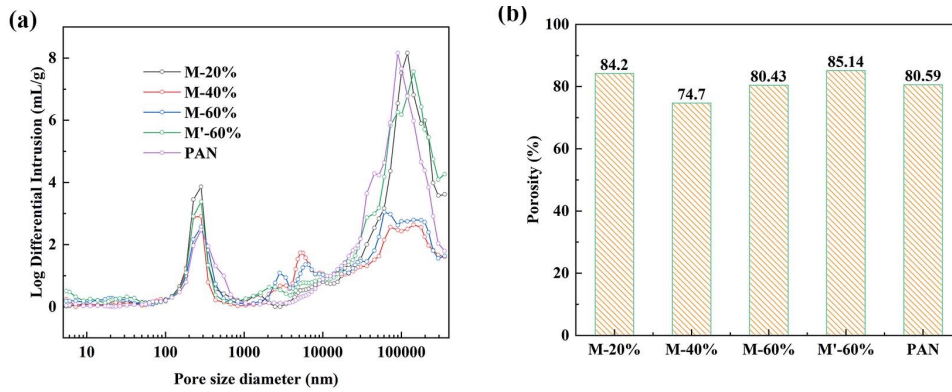## 13. Pore size and porosity of the obtained membranes

Fig S22 Pore size (a) and porosity (b) of the obtained membranes.

14. Adsorption isotherms and adsorption kinetics of M-60%

The DCF adsorption isotherms and kinetics experiment of M-60% were similar with MOF-808 powder, but replaced the powder absorbent with M-60% and recorded the mass of the membrane before adsorption experiments.

Table 5 Isothermal models parameters for DCF adsorption of M-60%

Parameters / Models	Adsorption isothermal parameters			
	$K_L(L \cdot mg^{-1})$	K_F	$Q_{max}(mg\ g^{-1})$	R^2
Freundlich		93.0		0.980
Langmuir	0.21		222	0.999

Table 6 Adsorption kinetic parameters of M-60% for DCF removal

Parameters / Model	kinetics parameters		
	$Q_e(mg \cdot g^{-1})$	K	R^2
Pseudo-first-order	119	0.27	0.989

Pseudo-second-order	124	0.00487	0.983

15. References

1. H. Furukawa, F. Gándara, Y.-B. Zhang, J. Jiang, W. L. Queen, M. R. Hudson and O. M. Yaghi, *J. Am. Chem. Soc.*, 2014, **136**, 4369-4381.

2. H.-L. J. Guorui Cai, *Angew. Chem. Int. Ed.*, 2017, **56**, 563 –567; P. Deria, J. E. Mondloch, E. Tylianakis, P. Ghosh, W. Bury, R. Q. Snurr, J. T. Hupp and O. K. Farha, *J. Am. Chem. Soc.*, 2013, **135**, 16801-16804.

3. Z. Hasan, N. A. Khan and S. H. Jhung, *Chem. Eng. J.*, 2016, **284**, 1406-1413.

4. S. Zhuang, R. Cheng and J. Wang, *Chem. Eng. J.*, 2019, **359**, 354-362.

5. S. Li, B. He, J. Wang, J. Liu and X. Hu, *Chemosphere*, 2020, **243**, 125343.

6. A. Karami, R. Sabouni and M. Ghommem, *J. Mol. Liq.*, 2020, **305**.

7. H. A. Younes, M. Taha, R. Mahmoud, H. M. Mahmoud and R. M. Abdelhameed, *J. Colloid Interface Sci.*, 2022, **607**, 334-346.

8. L. Zhang, B. Guo, H. He, X. Zhang, Y. Feng, W. Fan, J. Cao, G. Lu, Y. Chen, D. Sun and W. Huang, *Inorg. Chem.*, 2020, **59**, 695-704.

9. Z. Luo, S. Fan, J. Liu, W. Liu, X. Shen, C. Wu, Y. Huang, G. Huang, H. Huang and M. Zheng, *Polymers (Basel)*, 2018, **10**.

10. F. G. Quintero-Álvarez, C. K. Rojas-Mayorga, D. I. Mendoza-Castillo, I. A. Aguayo-Villarreal and A. Bonilla-Petriciolet, *Adsorpt Sci Technol*, 2022, **2022**.

11. W. Liu, X. Shen, Y. Han, Z. Liu, W. Dai, A. Dutta, A. Kumar and J. Liu, *Chemosphere*, 2019, **215**, 524-531.